Influence of Pendant Arms Bearing Ligating Groups on the Structure of Bismuth Porphyrins: Implications for Labeling Immunoglobulins Used in Medical Applications

ARTICLE *in* BIOCONJUGATE CHEMISTRY · NOVEMBER 2004

Impact Factor: 4.51 · DOI: 10.1021/bc049844o · Source: PubMed

5 AUTHORS, INCLUDING:

Zakaria Halime
Université de Bretagne Occidentale
29 PUBLICATIONS **313** CITATIONS
SEE PROFILE

Mohammed Lachkar
Sidi Mohamed Ben Abdellah University, Facu…
122 PUBLICATIONS **808** CITATIONS
SEE PROFILE

Influence of Pendant Arms Bearing Ligating Groups on the Structure of Bismuth Porphyrins: Implications for Labeling Immunoglobulins Used in Medical Applications

Zakaria Halime,[†,‡] Lydie Michaudet,[†] Mohammed Lachkar,[‡] Pierre Brossier,[§] and Bernard Boitrel*[,†]

Institut de Chimie, Université de Rennes1, UMR CNRS 6509, 35042 Rennes Cedex, France, Faculté des Sciences Dhar El Mehraz, Laboratoire d'Analyses, d'Essais et d'Environnement (L.A.E.E), Université Sidi Mohammed Ben Abdellah, B.P. 1796 (Atlas), 30000 Fès, Morocco, and Laboratoire de microbiologie médicale et moléculaire, Facultés de médecine et pharmacie, Université de Bourgogne, 7 Bd Jeanne d'Arc, 21000 Dijon, France. Received July 2, 2004; Revised Manuscript Received September 3, 2004

The synthesis of two picket bismuth(III) porphyrins is reported, and their crystal structures are compared. The influence of the nature of the pickets, as well as their number, is discussed in terms of stability, kinetics of metalation, structure, and distortion of the porphyrin. Unexpectedly, the results indicate that the coordination sphere of bismuth is not affected by different types of distortion nor is the stability of the complex. For both types of complexes, the X-ray crystallography revealed that a single arm is actually in direct interaction with the bismuth cation, thereby allowing further functionalization on the porphyrin core as the linkage with immunoglobulins or anti-rabbit antibodies (both noted IgG), which have been used in diagnostic or therapeutic applications.

INTRODUCTION

Bismuth coordination has long been represented by bismuth citrate because of its activity in the treatment of gastric ulcers (*1*, *2*). Very recently, the structure of colloidal bismuth subcitrate has also been investigated in dilute acidic medium (*3*). Additionally, compounds containing radioactive isotopes of bismuth such as ^{213}Bi are now under investigation due to the potential of α-emitting nuclides in radioimmunotherapy (*4*, *5*). However, a major issue remains the stable in vivo binding of the metal to the ligand without any leakage because it has been shown, for instance, that the binding constant of bismuth to human serum albumin is 10^{11} and that its binding to transferrin is even stronger (*6*). Different types of cyclic structures have also been investigated as potential chelates of bismuth. Among them, one can cite crown-ethers, tetraazamacrocyles and porphyrins (*7*−*11*). Until the early 1980s, few reports dealing with the complexation of bismuth into porphyrins had been published, presumably because of their instability (*12*). On the other hand, during the past decade, various studies led to a better understanding of the coordination of bismuth in porphyrins, whether in organic or aqueous medium (*13*−*17*). Our group has also investigated the potential of picket porphyrins as bismuth chelates, targeting on one hand a better knowledge of the coordination of bismuth and on the other hand the preparation of bifunctional linkers ready to be linked on biological proteins such as immunoglobulins (IgG). We have published the solid-state structures of two related porphyrins (*18*, *19*), as well as an evaluation of the length of the picket bearing an ethyl ester group (*20*).

In this study, we report the detailed preparation of these two bismuth porphyrins, a precise comparison of the corresponding X-ray structures, its implications for the transformation of the initial chelates in several analogous bifunctional linkers, and their reactivity toward IgG by means of different spacers.

EXPERIMENTAL PROCEDURES

General. Unless otherwise stated, the analytical facilities were provided by the Université de Bourgogne (C.S.M.) in Dijon.^{1}H (500.13 or 300.14 MHz) and ^{13}C (125.05 or 75.47 MHz) NMR spectra were recorded on Bruker Avance DRX 500 or Avance 300 spectrometers and referenced with respect to the residual protonated solvents. Mass spectra were performed on a MS/MS ZABSpec TOF spectrometer at the University of Rennes I (C.R.M.P.O.). UV/vis spectra were recorded on a Varian Cary 1E spectrometer, λ/nm (10^{-3} ϵ, M^{-1} cm^{-1}). IR spectra were recorded on a Bruker IFS 66 spectrometer in cm^{-1}. All solvents (ACS for analysis) were purchased from Carlo Erba. THF was distilled over potassium metal. CH_2Cl_2 was used as received. Triethylamine was distilled over CaH_2. The starting materials were generally used as received (Acros, Aldrich) without any further purification. All reactions were performed under an argon atmosphere and monitored by TLC (silica, CH_2Cl_2/CH_3-OH). Column flash chromatography was performed on silica gel (Merck TLC-Kieselgel 60H, 15 μm). Immunoglobulins and anti-rabbit antibodies were purchased from Sigma.

Syntheses. α-*5,10,15,20-Tetrakis{2-[3-(ethoxycarbonyl)propionylamido] phenyl} Porphyrin,* ***1***. αααα-Tetra-*ortho*-aminophenyl Porphyrin (TAPP) (0.2 g, 0.3 mmol) was dissolved in 20 mL of freshly distilled THF under argon. Ten equivalents of anhydrous Et_3N was added, and the mixture was cooled to 0 °C. Ethyl succinyl chloride (5 equiv) was then added, and the solution was stirred overnight. Solvent was evaporated to dryness, and the residue was dissolved in a minimum amount of CH_2-

* Corresponding author. Fax: 02 2323 5637. Tel: 02 2323 5856. E-mail: Bernard.Boitrel@univ-rennes1.fr.
† Université de Rennes1.
‡ Université Sidi Mohammed Ben Abdellah.
§ Université de Bourgogne.

10.1021/bc049844o CCC: $27.50
Published on Web 10/30/2004

Cl_2 to be poured on a silica gel chromatography column. Product was eluted with a 0.1% CH_3OH/CH_2Cl_2 mixture and obtained in 93% yield (330 mg, 0.28 mmol). Microanalysis, $C_{68}H_{66}N_8O_{12}\cdot CH_3OH$, found (calcd): C, 68.25 (67.97); H, 4.44 (4.79); N, 9.33 (9.19)%. FAB-MS: *m/z* = 1187.8 $[M + H]^+$. FTIR (KBr, cm^{-1}): 1731 $(CO)_{ester}$, 1694 $(CO)_{amide}$. UV−vis (CH_2Cl_2, λ nm, 10^{-3} ϵ, M^{-1} cm^{-1}): 419 (337), 514 (20.9), 546 (5.8), 588 (6.7), 643 (3.7). ^1H NMR ($CDCl_3$, 323 K, 500 MHz): δ_H 8.86 (8H, s, β-pyr), 8.59 (4H, d, J = 7.1 Hz, aro), 8.00 (4H, d, J = 7.5 Hz, aro), 7.86 (4H, t, J = 7.6 Hz, aro), 7.55 (4H, t, J = 7.2 Hz, aro), 7.19 (4H, s, −NHCO), 3.44 (8H, br s, $-CH_2CH_3$), 2.18 (8H, t, J = 6.7 Hz, $-CH_2CH_2$), 1.70 (8H, br s, $-CH_2CH_2$), 0.79 (12H, br s, $-CH_2CH_3$), −2.59 (2H, s, −NH pyr). ^{13}C NMR ($CDCl_3$, 300 K, 125 MHz): δ_C 172.6, 170.1, 138.7, 135.4, 132.1, 130.3, 123.9, 122.9, 115.5, 60.7, 31.5, 29.0, 14.1.

α-*5,10,15,20-Tetrakis{2-[3-(ethoxycarbonyl)propionylamido] phenyl} Porphyrin Bismuth(III) Nitrate,* ***1BiNO$_3$***. In a 50 mL flask, **1** (26 mg, 0.02 mmol) was dissolved in 7 mL of pyridine. This solution was warmed to 55 °C before $Bi(NO_3)_3\cdot 5H_2O$ (100 mg, 0.2 mmol) was added. After the solution was heated for 2 h, the solvent was evaporated, and the residue was dissolved in a minimum amount of CH_2Cl_2 to be poured on a silica gel chromatography column. The product was eluted with a 1.2% CH_3OH/CH_2Cl_2 mixture and obtained in 85% yield (25 mg, 0.017 mmol). Microanalysis, $C_{68}H_{64}BiN_9O_{15}\cdot 2H_2O$, found (calcd): C, 55.16 (54.73); H, 4.47 (4.59); N, 8.27 (8.45)%. FAB-MS: *m/z* = 1393.8 $[M - NO_3]^+$. UV−vis (CH_2Cl_2, λ nm, 10^{-3} ϵ, M^{-1} cm^{-1}): 354 (42.4), 472 (176.9), 598 (9.8), 644 (8.3). FTIR (KBr, cm^{-1}): 1732 $(CO)_{ester}$, 1695 $(CO)_{amide}$, 1384 (NO_3), 991 (Bi−Np). ^1H NMR ($CDCl_3$, 300 K, 500 MHz): δ 9.24 (8H, s, β-pyr), 8.68 (4H, br s, aro), 8.22 (3H, br s, −NHCO), 8.13 (1H, br s, −NHCO), 7.89 (4H, m, aro), 7.90 (4H, t, aro), 7.56 (4H, br s, aro), 3.46 (2H, br s, $-\mathbf{CH_2}CH_3$), 3.32 (6H, br s, $-\mathbf{CH_2}CH_3$), 2.04 (8H, br s, $-CH_2CH_2$), 1.92 (8H, br s, $-CH_2CH_2$), 0.96 (3H, br s, $-CH_2\mathbf{CH_3}$), 0.87 (9H, s, $-CH_2\mathbf{CH_3}$). ^{13}C NMR ($CDCl_3$, 300 K, 125 MHz): δ_C 173.5, 170.8, 149.3, 140.4, 134.9, 133.5, 131.3, 130.6, 123.6, 123.1, 122.7, 119.3, 60.8, 31.5, 29.5, 14.1.

α-*5,10,15-Tris(2-(acetylamido)phenyl)-*α*-20-{2-[3-(ethoxycarbonyl)propionylamido] phenyl} Porphyrin,* ***3***. Compound **2** (0.37 g, 0.4 mmol), prepared as previously described, was dissolved in 30 mL of freshly distilled THF under argon. Ten equivalents of anhydrous Et_3N (0.3 mL, 4 mmol) was added, and the mixture was cooled to 0 °C. Ethyl succinyl chloride (21.60 μL, 0.15 mmol) was then added, and this mixture was stirred overnight. The solvent was evaporated to dryness, and the residue was dissolved in a minimum amount of CH_2Cl_2. The compound was purified by chromatography on a silica gel column. The product was eluted with a 0.8% CH_3OH/CH_2Cl_2 mixture and obtained in 92% yield (407 mg, 0.37 mmol). Microanalysis, $C_{56}H_{48}N_8O_6\cdot CH_3OH\cdot H_2O$, found (calcd): C, 70.02 (69.92); H, 5.14 (5.56); N, 10.83 (11.44)%. FAB−HRMS: calcd *m/z* = 929.3775 $[M + H]^+$, found 929.3763. FTIR (KBr, cm^{-1}): 1741 $(CO)_{ester}$, 1679 $(CO)_{amide}$. UV−vis (CH_2Cl_2, λ nm, 10^{-3} ϵ, M^{-1} cm^{-1}): 419 (337.4), 514 (17.5), 547 (4.4), 587 (5.5), 643 (1.6). ^1H NMR ($CDCl_3$, 300 K, 300 MHz): δ_H 8.87 (8H, s, β-pyr), 8.71 (4H, br s, aro), 7.8 (8H, br s, aro), 7.55 (4H, br s, aro), 6.97 (4H, s, −NHCO), 3.55 (2H, q, J = 6.4 Hz, $-\mathbf{CH_2}CH_3$), 2.19 (2H, br s, $-CH_2CH_2-$), 1.60 (2H, br s, $-CH_2CH_2-$), 1.30 (9H, br s, $-CH_3$), 0.87 (3H, t, J = 6.4 Hz, $-CH_2\mathbf{CH_3}$), −2.71 (2H, s, −NH pyr). ^{13}C NMR ($CDCl_3$, 300 K, 75 MHz): δ_C 135.1, 130.1, 123.2, 123.4, 121.9, 121.5, 80.0, 77.3, 60.6, 31.1, 28.5, 24.1.

α-*5,10,15-Tris(2-(acetylamido)phenyl)-*α*-20-{2-[3-(hydroxycarbonyl)propionylamido]phenyl} Porphyrin,* ***4***. Compound **3** (100 mg, 0.09 mmol) was dissolved in THF to which was added KOH in ethanol (0.09 mmol in 5 mL). The mixture was heated at 50 °C for 4 h, cooled, and evaporated. The crude product was filtered in ethylic ether dissolved in water. Upon addition of HCl (6 M), precipitation occurred. The solid was neutralized by washing with water. The yield was quantitative. Microanalysis, $C_{54}H_{44}N_8O_6\cdot CH_3OH\cdot H_2O$, found (calcd): C, 69.58 (69.46); H, 4.87 (5.30); N, 11.42 (11.78)%. HR-MS (ESI): *m/z* 939.3017 $[(M + K)^+$, 100%]. ^1H NMR (500 MHz, DMSO-d_6, 298 K): δ_H 11.85 (s, 1H, −COOH), 8.81 (br s, 2H, −NHCO), 8.78 (br s, 2H, −NHCO), 8.70 (s, 8H, β-pyr), 8.14 (d, J = 7.5 Hz, 4H, aro), 8.10 (d, J = 7.5 Hz, 2H, aro), 7.94 (d, J = 7.0 Hz, 4H, aro), 7.83 (t, J = 8 Hz, 4H, aro), 7.57 (t, J = 6.5 Hz, 4H, aro), 1.99 (t, J = 5 Hz, 2H, $-CH_2CH_2-$), 1.64 (br s, 2H, $-CH_2CH_2-$), 1.24 (s, 3H, $-CH_3$), 1.22 (s, 6H, $-CH_3$), −2.72 (s, 2H, −NH pyr).

α-*5,10,15-Tris(2-(acetylamido)phenyl)-*α*-20-{2-[3-(carboxylate)propionylamido]phenyl} Porphyrin Bismuth(III),* ***4Bi***. The procedure described for preparation of **1BiNO$_3$** was applied without the silicagel chromatography column. The reaction was instantaneous with 1.1 equiv of bismuth nitrate in pyridine at room temperature. The compound was precipitated in a THF/ethylic ether mixture. HR-MS (ESI): *m/z* 1129.2863 $[(M + Na)^+$, 100%]. UV−vis (CH_2Cl_2): λ_{max}/nm (log ϵ, dm^2 mol^{-1} cm^{-1}): 350 (4.8), 472 (13.5), 598 (1.7), 646 (1.5). FTIR (of crystals, KBr, cm^{-1}): 1670 (CO); 990 ρ(Bi−Np). ^1H NMR (500 MHz, DMSO-d_6, 300 K): δ_H 9.03 (d, J = 4.5 Hz, 2H, β-pyr), 9.03 (d, J = 4.5 Hz, 2H, β-pyr), 8.99 (d, J = 8 Hz, 6H, pyr), 8.97 (d, J = 5 Hz, 2H, β-pyr), 8.89 (d, J = 5 Hz, 2H, β-pyr), 8.72 (br s, 4H, aro), 8.55 (t, J = 7 Hz, 3H, pyr), 8.33 (br s, 1H, aro), 8.33−8.26 (m, 2H, aro), 8.07 (t, J = 6.6 Hz, 1H, aro), 7.99 (t, J = 7.8 Hz, 6H, pyr), 7.90 (m, 3H, aro), 7.73 (br s, 1H, aro), 7.45 (br s, 4H, −NHCO), 7.36 (t, J = 7 Hz, 2H, aro), 7.16 (m, 2H, aro), 1.87 (br s, 2H, $-CH_2-$), 1.63 (br s, 2H, $-CH_2-$), 1.49 (s, 9H, $-CH_3$).

α-*5,10,15-Tris{2-[3-(ethoxycarbonyl)propionamido]-phenyl)}:* α-*20-(2-Aminophenyl) Porphyrin,* ***5***. Under argon, 0.37 g (0.4 mmol) of porphyrin single trityl TAPP (TrTAPP) was dissolved in 30 mL of THF. Ten equivalents of triethylamine and 0.23 mL (1.6 mmol) of ethyl succinyl chloride were added. The mixture was stirred overnigth at room temperature. It was evaporated and dissolved again in methylene chloride. Two milliliters of trifluoroactic acid was added to this solution. After 30 min of stirring, the solution was neutralized with gaseous ammonia, purified by silica gel chromatography column, and eluted with 0.8% $MeOH/CH_2Cl_2$ (yield = 76%, 320 mg, 0.30 mmol). Microanalysis, $C_{62}H_{58}N_8O_9\cdot CH_3OH$, found (calcd): C, 69.53 (69.34); H, 4.61 (4.73); N, 10.27 (10.27)%. MALDI-TOF-MS: *m/z* = 1059.1 $[M + H]^+$. UV−vis (CH_2Cl_2): λ_{max}/nm (log ϵ, dm^2 mol^{-1} cm^{-1}): 419 (289); 514 (18.4); 548 (4.7); 588 (5.7); 643 (1.8). ^1H NMR (500 MHz, $CDCl_3$, 323 K): δ_H 9.01 (d, J = 4.5 Hz, 2H, β-pyr); 8.85 (s, 6H, β-pyr); 8.67 (d, J = 8.1 Hz, 2H, aro); 8.61 (d, J = 7.9 Hz, 1H, aro); 8.05 (d, J = 7.0 Hz, 1H, aro); 8.01 (d, J = 7.0, 2H, aro); 7.90−7.87 (m, 4H, aro); 7.66 (td, J = 1.5 Hz, J = 7.9 Hz, 1H, aro); 7.57 (t, J = 7.0 Hz, 1H, aro); 7.55 (t, J = 7.3 Hz, 2H, aro); 7.22 (td, J = 1.1 Hz, J = 7.4 Hz, 1H, aro); 7.17 (dd, J = 0.8 Hz, J = 8.1 Hz, 1H, aro); 7.09 (s, 3H, −NHCO); 3.64 (large s, 2H, $-NH_2$); 3.53 (m, 4H, $-\mathbf{CH_2}CH_3$); 3.36 (br q, J = 6.7 Hz, 2H, $-\mathbf{CH_2}CH_3$); 2.28−2.13 (m, 6H, $-CH_2CH_2$); 1.70−1.63 (m, 6H, $-CH_2CH_2$); 0.86 (t, J = 6.7 Hz, 6H, $-CH_2\mathbf{CH_3}$); 0.75 (t, J = 6.7 Hz, 3H, $-CH_2\mathbf{CH_3}$); −2.65 (s, 2H). ^{13}C NMR ($CDCl_3$, 300 K, 125 MHz): δ_C 172.5; 170.0; 146.8; 138.7;

135.4; 132.0; 131.8; 130.5; 130.2; 126.5; 123.7; 122.4; 122.3; 118.3; 117.9; 115.9; 115.0; 60.7; 31.7; 29.1; 29.0; 14.2; 14.1.

α-*5,10,15-Tris{2-[3-(ethoxycarbonyl)propionamido]-phenyl}:* α-*20-[2-(Acrylamido)phenyl] Porphyrin,* ***6***. Porphyrin **5** (110 mg, 0.1 mmol) was dissolved in 20 mL of THF under argon at room temperature. Triethylamine (0.2 mL) and acryloyl chloride (25 μL) were added to this solution. After 12 h of stirring, the mixture was evaporated, and the compound was purified by chromatography on a silica gel column. The desired compound was obtained in a 78% yield (78 mg, 0.07 mmol). Microanalysis, $C_{62}H_{58}N_8O_9 \cdot CH_3OH$, found (calcd): C, 68.66 (68.35); H, 5.45 (5.82); N, 9.26 (9.52)%. FAB-MS: $m/z = 1113.0$ $[M]^{+\bullet}$. UV−vis (CH_2Cl_2): λ_{max}/nm (log ϵ, $dm^2\ mol^{-1}\ cm^{-1}$): 419 (350.8); 513 (19.6); 547 (4.6); 587 (6.0); 642 (1.6). ^1H NMR (500 MHz, $CDCl_3$, 323 K): δ_H 8.88 (m, 8H, β-pyr); 8.74 (d, $J = 7.3$ Hz, 1H, aro); 8.62 (d, $J = 7.9$ Hz, 3H, aro); 8.02 (m, 4H, aro); 7.87 (m, 4H, aro); 7.57 (m, 4H, aro); 7.22 (s, 1H, −NHCO); 7.15 (s, 3H, −NHCO); 5.9 (d, $J = 16.8$ Hz, 1H, $-CHCH_2$); 5.2 (large s, 1H, $-CHCH_2$); 5.1 (d, $J = 16.8$ Hz, 1H, $-CHCH_2$); 3.42 (large s, 6H, $-CH_2CH_3$); 2.19 (m, 6H, $-CH_2CH_2$); 1.73 (large s, 6H, $-CH_2CH_2$); 0.78 (m, 9H, $-CH_2CH_3$); −2.55 (s, 2H). ^{13}C NMR ($CDCl_3$, 300 K, 125 MHz): δ_C 172.4; 169.9; 163.3; 147.5; 138.8; 135.4; 132.1; 130.9; 130.2; 127.4; 123.8; 122.7; 115.6; 60.5; 31.6; 29.1; 14.0.

α-*5,10,15-Tris{2-[3-(ethoxycarbonyl)propionamido]-phenyl}:* α-*20-{2-[3-(Carboxy)propionamido]phenyl}Porphyrin,* ***7***. Porphyrin **5** (140 mg, 0.13 mmol) was heated at 50 °C in ethanol. Succinic anhydride (27 mg, 0.26 mmol, 2 equiv) was added to this solution. The mixture was stirred for 48 h, an additional 2 equiv of succinic anhydride was added, and the mixture was stirred again for 3 h. The desired compound was purified by chromatography on a silica gel column and eluted with 6% of $MeOH/CH_2Cl_2$ (yield = 85%, 170 mg, 0.15 mmol). Microanalysis, $C_{66}H_{62}N_8O_{12} \cdot CH_2Cl_2$, found (calcd): C, 64.48 (64.68); H, 5.05 (5.18); N, 8.58 (9.01)%. FAB-MS: $m/z = 1159.0$ $[M]^{+\bullet}$. ^1H (500 MHz, $CDCl_3$, 323 K): δ_H 11.9 (large s, 1H, −OH); 8.84 (s, 8H, β-pyr); 8.5 (large s, 2H, aro); 8.44 (d, $J = 6.8$ Hz, 2H, aro); 8.05 (d, $J = 6.1$ Hz, 2H, aro); 8.00 (d, $J = 7.1$ Hz, 2H, aro); 7.86 (t, $J = 7.3$ Hz, 4H, aro); 7.80 (large s, 4H, −NHCO); 7.58 (m, 4H, aro); 4.02 (large s, 2H, $-CH_2CH_3$); 3.64 (large s, 2H, $-CH_2-CH_3$); 3.57 (large s, 2H, $-CH_2CH_3$); 2.17 (t, $J = 6.2$ Hz, 2H, $-CH_2CH_2$); 2.04 (large s, 6H, $-CH_2CH_2-$); 1.66 (large s, 4H, $-CH_2CH_2$); 1.61 (large s, 4H, $-CH_2CH_2$); 0.96 (s, 3H, $-CH_3$); 0.89 (s, 6H, $-CH_3$); −2.73 (s, 2H). ^{13}C NMR ($CDCl_3$, 300 K, 125 MHz): δ_C 172.9; 170.8; 170.2; 138.8; 138.6; 135.4; 132.1; 130.1; 124.3; 123.9; 123.2; 115.7; 60.9; 31.1; 29.2; 28.9; 14.1.

Cross-Linking Reactions with the IgG. The employed IgG was provided from an antiserum (whole molecule) developed in goat using rabbit IgG as the immunogen (Sigma product no. R-1131). The antiserum has been treated to remove lipoproteins. Only the protein concentration was determined (the antiserum contains 17.2 mg of specific IgG per milliliter). The F(ab)′ fragment was obtained after reduction of the disulfide bridges of F(ab)′2 fragment (Sigma product no. R-9130) resulting from pepsin-digested antiserum (Sigma product no. R-1131).

Different solutions were prepared to be employed in the linking experimental procedures.

Buffered Solution A. The solution contains 0.1 M sodium phosphate dihydrate ($NaH_2PO_4 \cdot 2H_2O$) and 5 mM ethylenediamine tetraacetic acid dihydrate ($H_4EDTA \cdot 2H_2O$) in distilled water. The pH of the solution was tuned to 6 by addition of sodium hydroxide.

Buffered Solution B. The solution contains 0.1 M sodium phosphate dihydrate ($NaH_2PO_4 \cdot 2H_2O$), 1 mM ethylenediamine tetraacetic acid dihydrate ($H_4EDTA \cdot 2H_2O$), and 1 mM sodium chloride in distilled water. The pH of the solution was tuned to 7.5 by addition of hydrochloric acid.

Buffered Solution C. The solution contains 50 mM sodium tetraborate decadihydrate ($Na_2B_4O_7 \cdot 10H_2O$) and 5 mM ethylenediamine tetraacetic acid dihydrate ($H_4EDTA \cdot 2H_2O$) in distilled water. The pH of the solution was tuned to 8.3 by addition of diluted chlorohydric acid.

N-Succinimidyl(4-iodoacetyl)aminobenzoic Acid (SIAB) Solution. SIAB (1.4 mg, 0.003 mmol) was dissolved in 1 mL of DMSO.

Solution of Porphyrin ***5***. Porphyrin **5** (1.2 mg) was dissolved in 0.12 mL of DMSO to obtain a concentration of 9.44 mM.

Solution of Porphyrin ***6***. Porphyrin **6** (3.7 mg, 50 equiv relative to the antibody) was dissolved in 0.38 mL of DMSO to obtain a concentration of 8.5 mM.

Coupling Reaction of Porphyrin 5 with Fab′ Fragments Activated with SIAB, Fab′−SIAB−5. SIAB solution (10 μL, 5 equiv/protein) was added to the solution of reduced IgG. The mixture was then incubated in the dark at room temperature during 1 h. This solution of the activated Fab′ was purified by gel filtration chromatography over a Sephadex G25 column and eluted with buffered solution C. To the solution of purified Fab′−SIAB, 38 μL of the solution of **5** (50 equiv/protein) was added. The mixture was incubated for 1 h in the dark at room temperature to allow complete coupling of the Fab′. The solution of the final conjugate was purified again by gel filtration chromatography over a Sephadex G25 column and eluted with buffered solution C. A second chromatography did not change the ratio porphyrin/antibody.

Coupling Reaction of Porphyrin 6 with a Reduced IgG Fragment, Fab′−6. As a test reaction, the same porphyrin has been coupled with thiophenol, and the resulting porphyrin led to consistent analytical data. In a hemolysis tube, 2.5 mg of IgG was dissolved in 1 mL of buffered solution A. 2-Mercaptoethanolamine (MEA, 6.6 mg) was added, leading to a MEA concentration of 50 mM. The mixture was then stirred at 37 °C for 1 h, 30 min. Buffered solution B (2.5 mL) was added, and the Fab′ fragments were purified by gel filtration chromatography over a Sephadex G25 column (NAP-10 Pharmacia, Sweden). The reduced IgG were dissolved in 2.5 mL of buffered solution B, and 100 μL of solution of porphyrin **6** was added; then the mixture was stirred at room temperature. The conjugate was purified by gel filtration chromatography over a Sephadex G25 column and eluted with buffered solution B.

Coupling Reaction of Porphyrin 7 with Anti-Rabbit Antibodies, Ab−7. Porphyrin **7** was dissolved in THF together with *N*-hydroxysuccinimide and dicyclohexylcarbodiimide (DCC) under an argon atmosphere. After 24 h of stirring, the reaction mixture was filtered to remove the precipitate due to formation of DCU, evaporated and used without any further purification. The activated porphyrin was dissolved in DMSO, and 50 equiv/protein was employed. The same experimental procedure as above was applied.

RESULTS AND DISCUSSION

Obviously, the porphyrinic macrocycle is attractive owing to its coordination properties but also because it

Scheme 1: Synthetic Pathway for the Preparation of Succinylamido Picket Porphyrins[a]

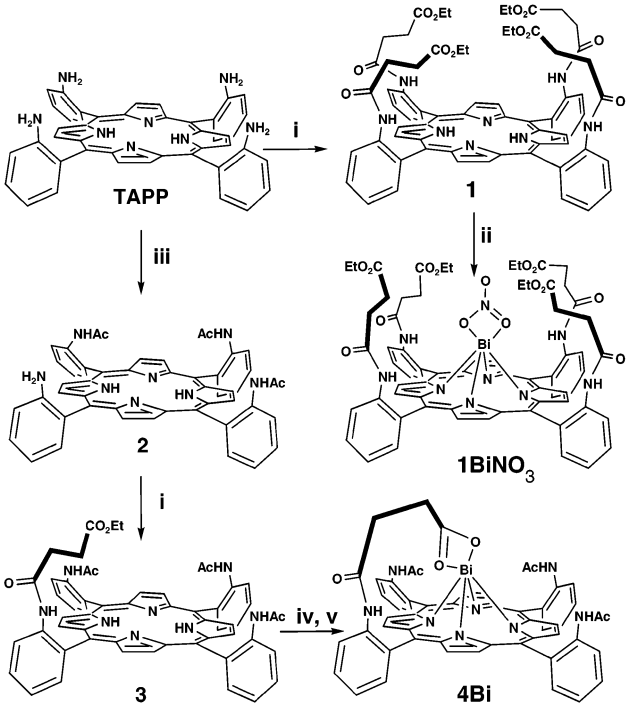

[a] Reagents and conditions: (i) $ClCO(CH_2)_2CO_2Et$ (5 equiv for **1** or 1.1 equiv for **3**), NEt_3, THF; (ii) $Bi(NO_3)_3{\cdot}5H_2O$ (10 equiv), 55 °C, pyridine, 2 h; (iii) CH_3COCl (3 equiv), NEt_3, THF; (iv) KOH, EtOH, 55°C → **4**; (v) $Bi(NO_3)_3{\cdot}5H_2O$ (1.2 equiv), rt, pyridine, 10 min.

represents a relatively rigid and disk-shaped structure suitable as a framework to build up new types of artificial chelators. Furthermore, meso-ortho-substituted phenyl porphyrins, owing to their possible atropisomerization, provide another interesting property that allows preorganization on a specific side of the macrocycle. We have taken advantage of this particularity by performing very simple reactions on αααα-tetra-*ortho*-aminophenyl porphyrin (TAPP). The initial idea consisted in supplementing the porphyrin by four ester pickets, assuming that one or several pickets would bend over the porphyrin ring to complete and satisfy the coordination sphere of the metal, making it inaccessible to dissociation (*21*). Besides, in compound **1BiNO$_3$**, the picket fence could protect the metal from any intermolecular interaction. In a second step, we have prepared the single carboxylic acid picket porphyrin **4**, keeping in mind that, bismuth being trivalent, the carboxylate function would lead to a neutral complex. The synthesis of these two ligands is detailed in Scheme 1.

Where porphyrin **1** bearing four ethyl succinyl pickets (4ES) is obtained by a straigthfoward acylation of the αααα atropisomer of TAPP with ethyl succinyl chloride, the preparation of **4** requires several extra steps to reach the single succinic acid compound (1SA). Indeed, the first step of the synthesis requires the protection of three amino groups of TAPP with acetyl chloride in dry THF. The optimization of the yield (55%) toward the three-protected porphyrin **2** requires the use of 3 equiv of the acylation reagent, and the separation of undesired compounds such as the tetra- and diacylated porphyrins was performed on a silica gel chromatography (*20*). The remaining amino group was functionalized with 1.1 equiv of ethyl succinyl chloride to obtain **3** (89%) the ester group of which was hydrolyzed with KOH, leading to **4**. So far, we performed the metal insertion by heating at 50 °C

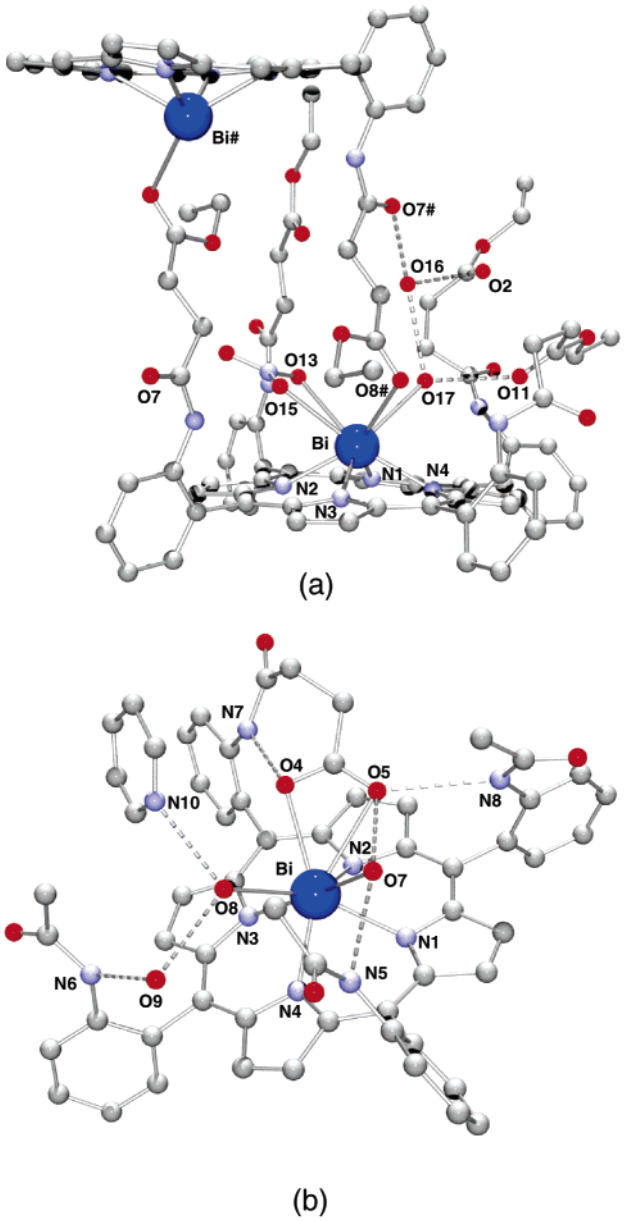

Figure 1. Ball and stick representation of the crystal structure of (a) **1BiNO$_3$** and (b) **4Bi**.

the free-base porphyrin with bismuth nitrate in pyridine. Actually, we found out that this complexation is achieved after stirring for 10 min at room temperature. Both complexes led to an X-ray structure, and the detailed comparison of these structures (Figure 1) is instructive both in terms of differences and similarities.

In both complexes, the Bi(III) is eight coordinate with an approximate square antiprismatic geometry. One square is formed by the four nitrogen atoms from the porphyrin, the other one being composed of four oxygen atoms. Two of them come from the bidentate counteranion, whether nitrate in **1BiNO$_3$** or carboxylate for **4Bi**. The third bound oxygen atom comes from a water molecule included in a hydrogen bonding net: O17 in **1BiNO$_3$**; O7 in **4Bi**. In **1BiNO$_3$**, the fourth bound oxygen comes from a carbonyl oxygen atom O8# of the terminal ester group belonging to an arm attached to a symmetrically related macrocycle, forming in this way, a centrosymmetric dimer. For **4Bi**, which exhibits a mononuclear structure—the first major difference between the two structures, a second water molecule represents the fourth oxygen atom O8. For both compounds, only one

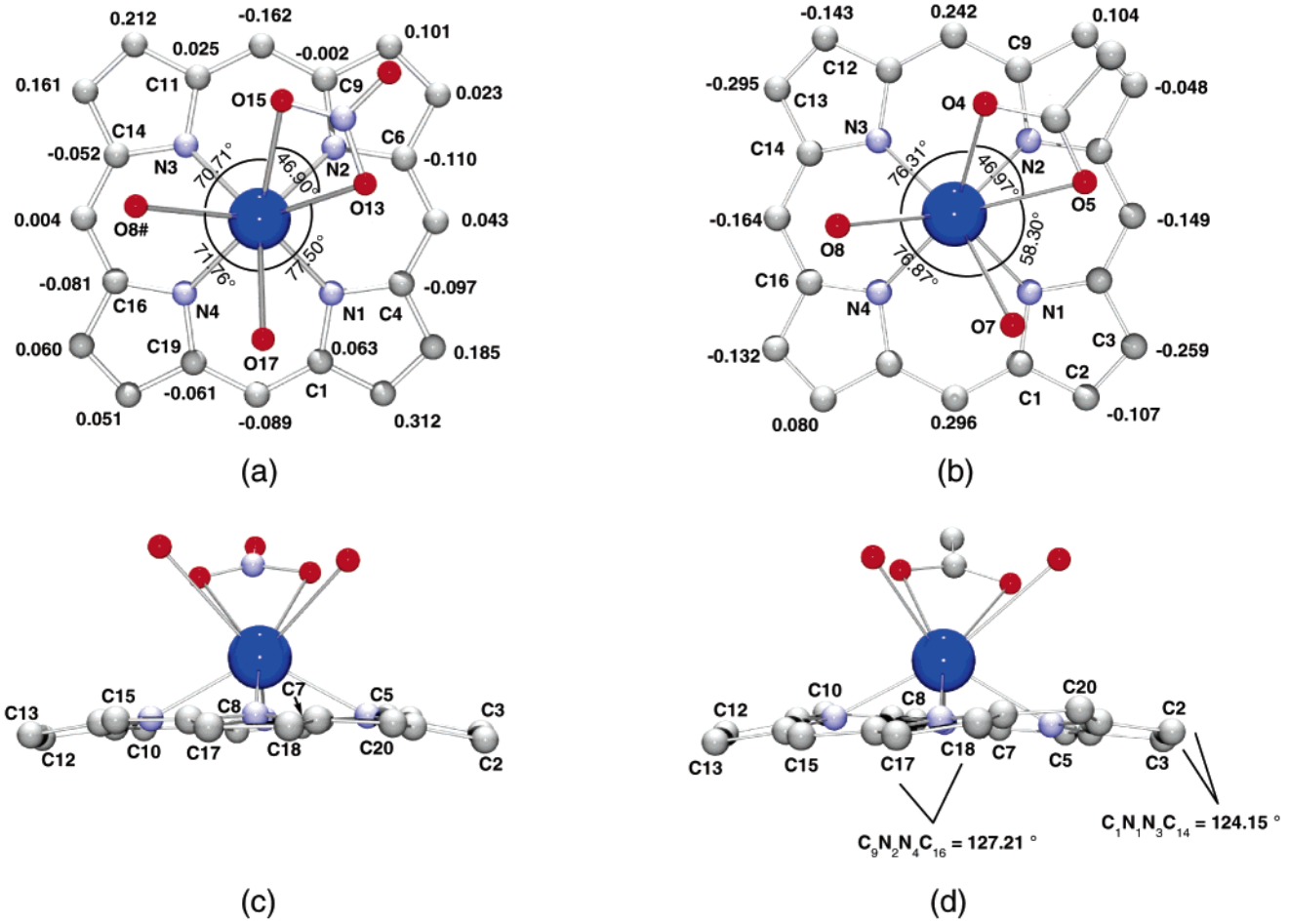

Figure 2. Ball and stick polyhedron coordination top views of (a) **1BiNO$_3$** and (b) **4Bi** and side views of (c) **1BiNO$_3$** and (d) **4Bi**. All the deviations refer to the mean porphyrin plane.

arm is in direct interaction with the metal, either in an intermolecular fashion in **1BiNO$_3$** or in an intramolecular scorpionate-like coordination in **4Bi**. Indeed, for the dimer, two other ester pickets are taking part to the hydrogen bonding net including the water molecule O17. But the fourth picket seems to have no function in the stability of the complex: this detail is worth underlining and will be discussed later in terms of further functionalization of the ligand. In the monomer, the amide function from the three acetyl pickets belongs to the hydrogen bonding net, which also includes the two bismuth-bound water molecules O7 and O8. However, the major driving force of this structure is undoubtely the carboxylate group, which binds in a bidentate fashion the metal, occupying two coordination sites and leading to a neutral complex. In organic solvents, this tailed carboxylate group allows porphyrin **4** to complex bismuth almost instantaneously. This represents a significant improvement in the kinetics of metalation relative to its ester picket analogue for which heating the ligand at 50 °C was necessary to obtain a complete metalation (*20*).

In both structures, the bismuth cation is largely displaced out of the N_4 plane of the porphyrin, 1.125 and 1.145 Å in **1BiNO$_3$** and **4Bi**, respectively. In the binuclear structure of **1BiNO$_3$**, the intermetallic distance is 10.61 Å. Our preliminary study was in favor of a monomeric structure in solution (*20*). However, this conclusion was reached for the compound dissolved in an organic solvent. In terms of therapeutic applications, and so in aqueous medium, if this binuclear edifice was maintained, it would be possible to deliver not one but two radioactive nuclei per complex. This would represent a simple and efficient method to directly increase the amount of α particles around the targeted cells.

Two other significant differences between these two complexes are exhibited in Figure 2, which outlines the coordination sphere of bismuth (panels a and b), as well as a side view of the porphyrin plane (panels c and d). The first one concerns the antiprismatic coordination sphere, which is almost regular in **1BiNO$_3$** but severly distorted in **4Bi**. For example, the angle in the dimer between O13−Bi and Bi−O17 is 77.5°, but the angle is only 58.3° in the monomer between O5−Bi and Bi−O7. A possible explanation for this distortion in which a labile water molecule takes part could be that O7, to be stabilized, requires being equidistant between O5 and N5, but the length of the hydrogen bonds O5−O7 (2.821 Å) and O7−N5 (3.053 Å) are not very consistent with this explanation. In fact, the angle between the oxygen atom−Bi bonds of the bidentate ligand is the only one to be identical in the two complexes.

The second main distortion to be observed concerns the porphyrin core itself. Indeed, porphyrins are known to adopt various conformations according to the bound metal and the steric hindrance or the electronic properties of its substituents. Chiefly, to identify this distortion, the displacement of the four meso carbon atoms, as well as the eigth β-pyrrolic carbon atoms, in respect to the 24 atom mean porphyrin plane is calculated. The mean porphyrin plane refers to the least-squares mean plane calculated for the 24 atom macrocycle and not that for the four coordinating nitrogen atoms, the metal being not included in the calculations. The Cα−N−N−Cα torsion angle is also taken into account to quantify the degree

of ruffling. According to these displacements, it appears that the porphyrin in the dimer is domed (*22*, *23*), whereas it is both ruffled (*24*, *25*) and saddled (*26*, *27*) in the monomer. The former distortion is quite usual in most of the previously reported X-ray structures of bismuth porphyrins (*15*, *17*) and could be attributed to the out-of-plane coordination of the metal itself. Typically, the domed conformation is only observed when the porphyrin is coordinated to a large central metal ion, usually with one or more axial ligands. Indeed, in Figure 2a, it is clear that all the β carbons are on one side (below with a positive displacement) of the porphyrin mean plane where the meso carbons are in or near the plane. All the α carbons but two, C1 and C11, and the nitrogens are located above the mean porphyrin plane with negative displacements, on the same side as the metal (*28*).

On the other hand, the unusual mixed conformation of the monomer is presumably due to the nonsymmetrical substitution pattern of the porphyrin. Indeed, the carbon atoms in the opposite meso positions (5,15 and 10,20) are not located in the 24-atom least-squares plane but above or below. More precisely, the deviations (Cm) from the mean porphyrin plane of these atoms are 0.296, −0.149, 0.242, and −0.164 Å, leading to an average absolute value of 0.213 Å. This is expected for a ruffle conformation and not for a saddled macrocycle. But in the former conformation, the β carbons of the same pyrrolic subunit should be on opposite sides of the porphyrin mean plane. This distribution is not regularly observed for **4Bi** because C2 and C3 as well as C12 and C13 are located on the same side of the macrocyle. However, the torsion angles C9N2N4C16 and C1N1N3C14 are found to be equal to 127.21° and 124.15°, respectively, representing the signature of a ruffled macrocycle. Moreover, the tilts of the pyrrole planes against each other are 8° and 17°, confirming clearly this significant ruffling. This conformation has been found in porphyrins with small metal ions such as Ni(II) owing to the Ni−N bond shortening (*29*, *30*) but to the best of our knowledge was unkown for a large cation with a crystalline radius of 1.31 Å (for a coordination of 8) (*31*). These two major distortions seem also to be the result of a too short length of the coordinating arm because the latter has to pull the meso carbon on which it is tethered to be able to coordinate the metal. Nevertheless, it is worth noting that **4Bi**, bearing a single coordinating picket and exhibiting significative distortions, is as stable as **1BiNO$_3$** in organic solvents. Of course, this situation may be altered in aqueous medium because our final objective remains to link these chelates on a protein. A direct consequence of this observation is that by replacing the succinyl motif by a longer coordinating arm it should be possible to obtain an even more stable complex with a planar, or at least a less distorted, porphyrin core.

In light of both X-ray structures, we have verified that this type of porphyrin could be further functionalized without interfering with the key features of the coordination sphere. This is the reason, as a test reaction, we have chosen to transform ligand **1** in a bifunctional linker (*32*) ready to react with immunoglobulins (IgG). Indeed, for future applications with the radioactive isotope, the free carrier, and not the metalled complex, will be attached to the IgG.

As earlier mentioned, in **1BiNO$_3$**, only one picket does not seem to be decisive in the stability of the complex. We reasoned that this ethylsuccinyl picket could be replaced by a linker properly designed without perturbing considerably the coordination properties of the ligand. The synthesis consists of sparing one amino function of TAPP by employing the single trityl TAPP (TrTAPP), prepared as previously described (*33*). The further steps then introduce a reactive function for either primary amines of the lysine residues or thiol groups from the cysteine and particularly those obtained after reduction of the disulfide bridges of immunoglobulins, which leads to the Fab′ fragments (Scheme 2) (*34*). The reaction targeting coupling with thiol groups of the Fab′ was performed from the reduced fragment of the IgG obtained according to the usual methodology with 2-mercaptoethanolamine. Thus, porphyrin **5**, easily synthesized from TrTAPP and bearing only three succinyl pickets, was transformed in porphyrin **6** and porphyrin **7** by reaction with acryloyl chloride and succinic anhydride, respectively. In the first case, the sulfhydryl groups of the reduced IgG are known to react with the acrylamide function according to a 1,4 addition creating a stable thioether bond (*34*). In the second case, the resulting porphyrin **7** bearing a four-carbon spacer was activated by the *N*-hydroxysuccinimide (NHS) method and then coupled with the complete IgG via formation of amide bonds. Because of the lack of precise methods such as γ emission counting, only a rough evaluation of the porphyrin/IgG ratios was possible. Indeed, because the porphyrin absorbs around 420 nm with an average ϵ of 350 000 M^{-1} cm^{-1} and the protein (IgG) absorbs at 280 nm with an ϵ = 195 000 M^{-1} cm^{-1}, this evaluation was performed by UV−visible spectroscopy. This methodology has already been successfully employed with a sulfonated aluminum phthalocyanine bearing a 6-aminohexanoic acid spacer and a murine anti-CEA monoclonal antibody (*35*). Additionally, in our case, it is also expected to be convenient for future in vivo studies with the bismuth complex, which absorbs at 470 nm.

A typical UV−visible spectrum is illustrated by the coupling of porphyrin **7** to an antibody (Figure 3). The molar protein concentration, C_{ab}, and molar porphyrin concentration, C_p, are given by the following equations: $A_{280\ nm}/(l\epsilon_{ab}) = C_{ab}$ and $A_{428\ nm}/(l\epsilon_p) = C_p$. This calculation allows one to obtain an approximate number of dye molecules per antibody molecule.

We first investigated the coupling of porphryin **6** to Fab′ fragments. With an excess of 50 equiv of this porphyrin and ϵ_p = 350 800 M^{-1} cm^{-1}, only 40% of the Fab′ were found to be conjugated to the porphyrin. When the excess of porphyrin was decreased to 25 equiv, only 15% of the Fab′ were labeled. The same type of measurement was performed to evaluate the coupling between IgG and porphyrin **7** according to the activated ester method, but the result was as disapointing as that for the previous one. Indeed, only 20% of the protein was linked to the porphyrin. In fact, although the two reactions cannot be compared, these two results are consistent with one another and could be explained by a too short length of the spacers (3−4 atom-length). Indeed, it has been reported that the approach of the reactive functions from the antibodies can be sensitive to the steric hindrance of the chelate (*36*).

This prompted us to reinvestigate this conjugation by using a commercially available spacer. We have chosen the *N*-succinimidyl(4-iodoacetyl)aminobenzoic acid (SIAB) for two reasons. First, the length of this spacer is greater than the two previous ones with a value of 10.6 Å. Second, the activated ester function of the spacer allows the direct coupling of the Fab′ on porphyrin **5** without any other reaction or purification step on it. The iodoactetyl function of this heterobifunctional cross-linker will react with the thiol groups of the reduced IgG (Fab′). According to the same method, the ratio C_p/C_{ab} is found to equal 1.5.

Scheme 2: Synthesis of Different Bifunctional Ligands Related to 1 and Their Coupling with an Antibody (Ab) or Reduced Antibody (Fab′)[a]

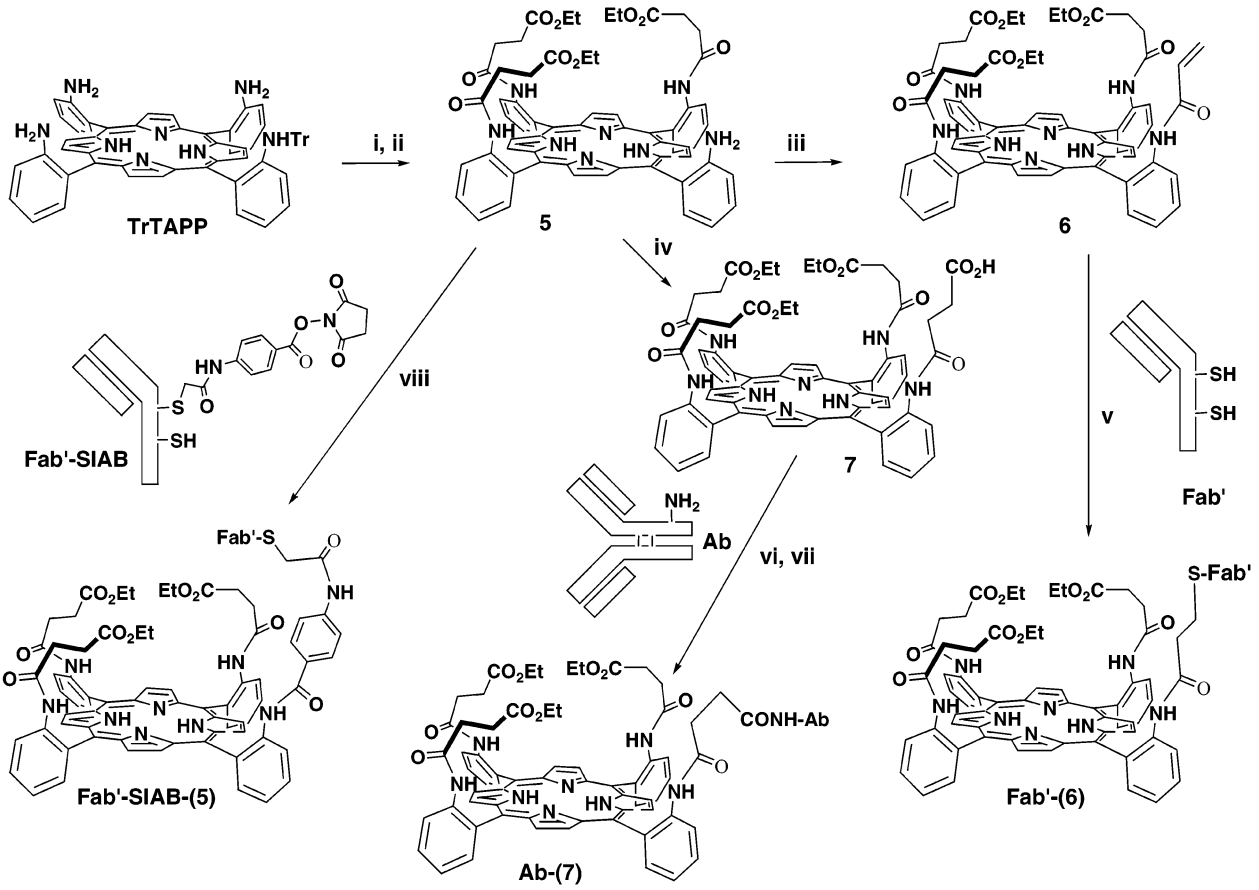

[a] Reagents and conditions: (i) $ClCO(CH_2)_2CO_2Et$ (4 equiv), NEt_3, THF; (ii) TFA, CH_2Cl_2; (iii) $ClCOCH{=}CH_2$ (1.5 equiv), NEt_3, THF; (iv) succinic anhydride (2 equiv), EtOH, 50 °C, 48 h; (v) reduced antibody (Fab′); (vi) NHS/DCC; (vii) antibody; (viii) SIAB-activated reduced antibody.

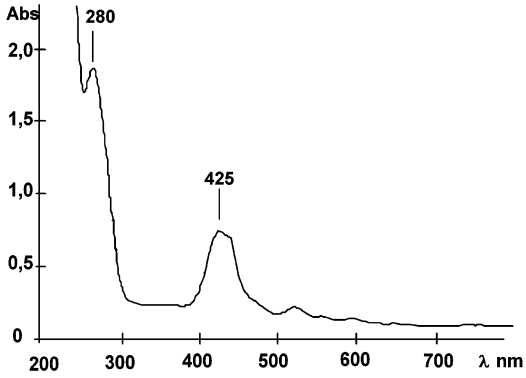

Figure 3. UV−vis spectrum of the immunoconjugate **Ab**−**7**.

If one considers that the Fab′ is completely labeled, 50% is attached to one porphyrin whereas the other 50% is doubly marked. This third coupling test reaction clearly indicates that with a chelate such as picket porphyrins, the length of the linker becomes critical in comparison with other ligands such as nonaromatic tetraazamacrocycles.

CONCLUSIONS

In summary, we have shown that both bismuth complexes for which the solid-state structures are known are valid molecules for further investigations in radioimmunotherapy applications. For the dimeric complex, three pickets among the four available are included in the structure of the complex. Interestingly, if the dimeric structure is maintained in aqueous medium with the hot radioisotope, this type of edifice could carry two radioactive nuclei instead of one, thereby delivering a higher dose of high linear energy emission. For the monomer, the scorpionate built-in tail guarantees the neutrality of the complex without any exogenous counteranion and a faster complexation of the bismuth. Various bifunctional chelates have been synthesized by introducing usual reactive groups for linking these ligands with immunoglobulins (IgG) or reduced IgG (Fab′). Our results indicate that the length of the spacer between the chelate and the IgG or reduced IgG is a crucial parameter. Work is in progress to investigate the immunological properties of these conjugates toward the rabbit IgG immunogen before and after the complexation of the radioactive isotope of bismuth.

ACKNOWLEDGMENT

We gratefully acknowledge La Ligue contre le cancer, Région Bretagne, and the CNRS for financial support. We are particularly indebted to the Comité des Côtes-d′Armor de La Ligue contre le cancer for his generous help to Z.H.

LITERATURE CITED

(1) Herrmann, W. A., Herdtweck, E., and Pajdla, L. (1991) "Colloidal Bismuth Subcitrate" (CBS): Isolation and Structural Characterization of the Active Substance against *Helicobacter pylori*, a causal Factor of Gastric Diseases. *Inorg. Chem. 30*, 2579−2581.

(2) Asato, E., Katsura, K., Mikuriya, M., Fujii, T., and Reedijk, J. (1993) Synthesis, Structure, and Spectroscopic Characterization of Bismuth Citrate Compounds and Bismuth-Containing Ulcer Healing Agent Colloidal Bismuth Subcitrate (CBS). 3. Crystal and Solution Structures of $K(NH_4)[Bi_2(cit)_2(H_2O)_2]\cdot(H_2O)_x$ ($x = 2, 4$). *Inorg. Chem. 32*, 5322−5329.

(3) Li, W., Jin, L., Zhu, N., Hou, X., Deng, F., and Sun, H. (2003) Structure of Colloidal Bismuth Subcitrate (CBS) in Dilute HCl: Unique Assembly of Bismuth Citrate Dinuclear Units ($[Bi(cit)_2Bi]^{2-}$). *J. Am. Chem. Soc. 125*, 12408−12409.

(4) Brechbiel, M. W., Gansow, O. A., Pippin, C. G., Rogers, R. D., and Planalp, R. P. (1996) Preparation of the Novel Chelating Agent *N*-(2-Aminoethyl)-*trans*-1,2-diaminocyclohexane-*N*,*N*′,*N*″-pentaacetic Acid $(H_5CyDTPA)^{2-}$ and $Bi^{III}(H_2$-DTPA) Complexes. *Inorg. Chem. 35*, 6343−6348.

(5) Yao, Z., Zhang, M., Garmestani, K., Axworthy, D. B., Mallett, R. W., Fritzberg, A. R., Theodore, L. J., Plascjak, P. S., Eckelman, W. C., Waldmann, T. A., Pastan, I., Paik, C. H., Brechbiel, M. W., and Carrasquillo, J. A. (2004) *Clin. Cancer Res. 10*, 3137−3146.

(6) Sun, H., and Szeto, K. Y. (2003) Binding of bismuth to serum proteins: implication for targets of Bi(III) in blood plasma. *J. Inorg. Biochem. 94*, 114−120.

(7) Alcock, N. W., Ravindran, M., and Willey, G. (1989) Crown Ether Complexes of Bi^{III}. Synthesis and Crystal and Molecular Structures of $BiCl_3$.12-Crown-4 and $2BiCl_3$.18-Crown-6. *J. Chem. Soc., Chem. Commun.* 1063−1064.

(8) Rogers, R. D., Bond, A. H., Aguinaga, S., and Reyes, A. (1992) Complexation Chemistry of Bismuth(III) Halides with Crown Ethers and Polyethylene Glycols. Structural Manifestations of a Stereochemically Active Lone Pair. *J. Am. Chem. Soc. 114*, 2967−2977.

(9) Luckay, R., Reibenspies, J. H., and Hancock, R. D. (1995) Synthesis and Structure of a Complex of Bismuth(III) with a Nitrogen Donor Macrocycle. *J. Chem. Soc., Chem. Commun.* 2365−2366.

(10) Luckay, R., Cukrowski, I., Mashishi, J., Reibenspies, J. H., Bond, A. H., Rogers, R. D., and Hancock, R. D. (1997) Synthesis, stability and structure of the complex of bismuth-(III) with the nitrogen-donor macrocycle 1,4,7,10-tetraazacyclododecane. The role of the lone pair on bismuth(III) and lead(II) in determining coordination geometry. *J. Chem. Soc., Dalton Trans.* 901−908.

(11) Buchler, J. W., and Lay, K. L. (1974) Arsen-, Antimon- und Wismutkomplexe des Octaäthylporphins. *Inorg. Nucl. Chem. Lett. 10*, 297−300.

(12) Treibs, A. (1969) Metallkomplexe von Porphyrinen. *Justus Liebigs Ann. Chem. 728*, 115−148.

(13) Sayer, P., Gouterman, M., and Connell, C. R. (1982) Metalloid Porphyrins and Phathalocyanines. *Acc. Chem. Res. 15*, 73−79.

(14) Barbour, J., Belcher, W. J., Brothers, P. J., Rickard, C. E. F., and Ware, D. C. (1992) Preparation of Group 15 (Phosphorus, Antimony, and Bismuth) Complexes of *meso*-Tetra-*p*-tolylporphyrin (TTP) and X-ray Crystal Structure of $[Sb(TTP)(OCH(CH_3)_2)_2]Cl$. *Inorg. Chem. 31*, 746−754.

(15) Michaudet, L., Fasseur, D., Guilard, R., Ou, Z., Kadish, K. M., Dahoui, S., and Lecomte, C. (2000) Synthesis, characterization and electrochemistry of bismuth porphyrins. X-ray crystal structure of $(OEP)Bi(SO_3CF_3)$. *J. Porphyrins Phthalocyanines 4*, 261−270.

(16) Chacko, G.-P., and Hambright, P. (1994) Acid-, Anion-, and Base-Catalyzed Solvolysis Reactions of a Water Soluble Bismuth(III) Porphyrin. *Inorg. Chem. 33*, 5595−5597.

(17) Boitrel, B., Breede, M., Brothers, P. J., Hodgson, M., Michaudet, L., Rickard, C. E. F., and Al Salim, N. (2003) Bismuth porphyrin complexes: syntheses and structural studies. *Dalton Trans.* 1803−1807.

(18) Michaudet, L., Richard, P., and Boitrel, B. (2000) Synthesis and crystal structure of an unprecedented bismuth porphyrin containing ester pendant arms. *Chem. Commun.* 1589−1590.

(19) Boitrel, B., Halime, Z., Michaudet, L., Lachkar, M., and Toupet, L. (2003) Structural characterisation of the first mononuclear bismuth porphyrin. *Chem. Commun.* 2670−2671.

(20) Halime, Z., Michaudet, L., Razavet, M., Ruzié, C., and Boitrel, B. (2003) Synthesis, characterisation, and properties of bismuth(III) ester pendant arms picket porphyrins. *Dalton Trans.* 4250−4254.

(21) Hancock, R. D., Maumela, H., and S. de Sousa, A. (1996) Macrocyclic ligands with pendent amide and alcoholic oxygen donor groups. *Coord. Chem. Rev. 148*, 315−347.

(22) Ryu, S., Whang, D., Kim, J., Yeo, W., and Kim, K. (1993) Synthesis, Characterization and Crystal Structures of Novel Hafnium Porphyrins. *J. Chem. Soc., Dalton Trans.* 205−209.

(23) Dawson, D. Y., Brand, H., and Arnold, J. (1994) Tantalum Porphyrin Chemistry. Synthesis and Reactivity of Organometallic Derivatives and the X-ray Crystal Structure of the Sandwich Compound $[Ta(OEP)_2][TaCl_6]$. *J. Am. Chem. Soc. 116*, 9797−9798.

(24) Medforth, C. J., Senge, M. O., Smith, K. M., Sparks, L. D., and Shelnutt, J. A. (1992) Nonplanar Distortion Modes for Highly Substituted Porphyrins. *J. Am. Chem. Soc. 114*, 9859−9869.

(25) Senge, M. O., Ema, T., and Smith, K. M. (1995) Crystal structure of a remarkably ruffled nonplanar porphyrin (pyridine)[5,10,15,20-tetra(*tert*-butyl)porphyrinato]zinc(II). *J. Chem. Soc., Chem. Commun.* 733−734.

(26) Sparks, L. D., Medforth, C. J., Park, M. S., Chamberlain, J. R., Ondrias, M. R., Senge, M. O., Smith, K. M., and Shelnutt, J. A. (1993) Metal Dependence of the Nonplanar Distortion of Octaalkyltetraphenylporphyrins. *J. Am. Chem. Soc. 115*, 581−592.

(27) Barkigia, K. M., Renner, M. W., Furenlid, L. R., Medforth, C. J., Smith, K. M., and Fajer, J. (1993) Crystallographic and EXAFS studies of conformationally designed nonplanar nickel(II) porphyrins. *J. Am. Chem. Soc. 115*, 3627−3635.

(28) For an interactive introduction to porphyrin distortions and more details about the deviations of each atom, see: http://www-chem.ucdavis.edu/groups/smith/chime/chime_index.html.

(29) Brennan, T. D., Scheidt, W. R., and Shelnutt, J. A. (1988) New crystalline phase of (octaethylporphinato)nickel(II): effects of π-π interactions on molecular structure and resonance Raman spectra. *J. Am. Chem. Soc. 110*, 3919−3924.

(30) Richard, P., Rose, E., and Boitrel, B. (1998) Characterization and crystal structure of a chiral ruffled basket-handle porphyrin. *Inorg. Chem. 37*, 6532−6534.

(31) Shannon, R. D. (1976) Revised Effective Ionic Radii and Systematic Studies of Interatomic Distances in Halides and Chalcogenides. *Acta Crystallogr. A32*, 751−753.

(32) Liu, S., and Edwards, D. S. (2001) Bifunctional chelators for therapeutic lanthanide radiopharmaceuticals. *Bioconjugate Chem. 12*, 7−34.

(33) Collman, J. P., Bröring, M., Fu, L., Rapta, M., Schwenninger, R., and Straumanis, A. (1998) Novel protecting strategy for the synthesis of porphyrins with different distal and proximal superstructures. *J. Org. Chem. 63*, 8082−8083.

(34) Hermanson, G. T. (1996) *Bioconjugate Techniques*, Academic Press, New York.

(35) Carcenac, M., Larroque, C., Langlois, R., Van Lier, J. E., Artus, J. C., and Pèlegrin, A. (1999) Preparation, Phototoxicity and Biodistribution Studies of Anti-Carcinoembryonic Antigen Monoclonal Antibody-Phthalocyanine Conjugates. *Photochem. Photobiol. 70*, 930−936.

(36) Bedel-Cloutour, C. H., Maneta-Peyret, L., Pereyre, M., and Bezian, J. H. (1991) Synthesis of a Monoclonal Antibody-Indium-111-Porphyrin Conjugate. *J. Immunol. Methods 144*, 35−41.

BC049844O